HHS Public Access

Author manuscript

J Control Release. Author manuscript; available in PMC 2019 November 28.

Published in final edited form as:

J Control Release. 2018 November 28; 290: 75–87. doi:10.1016/j.jconrel.2018.09.025.

Potent *in vivo* lung cancer Wnt signaling inhibition *via* cyclodextrin-LGK974 inclusion complexes

Pedro P.G. Guimaraes[a,b,c,d], **Mingchee Tan**[a,b], **Tuomas Tammela**[a,1], **Katherine Wu**[a,1], **Amanda Chung**[a,b], **Matthias Oberli**[a,b], **Karin Wang**[e], **Roman Spektor**[f], **Rachel S. Riley**[d], **Celso T.R. Viana**[g], **Tyler Jacks**[a], **Robert Langer**[a,b,*], and **Michael J. Mitchell**[d,**]

[a] Koch Institute for Integrative Cancer Research, MIT, Cambridge, MA, United States

[b] Department of Chemical Engineering, MIT, Cambridge, MA, United States

[c] Department of Physiology and Biophysics, Institute of Biological Sciences, Universidade Federal de Minas Gerais, Belo Horizonte, MG, Brazil

[d] Department of Bioengineering, University of Pennsylvania, Philadelphia, PA, United States

[e] Department of Bioengineering, Temple University, Philadelphia, PA, United States

[f] Graduate Field of Genetics, Genomics and Development, Cornell University, Ithaca, NY, United States

[g] Department of General Pathology, Institute of Biological Sciences, Universidade Federal de Minas Gerais, Belo Horizonte, MG, Brazil

Abstract

Activation of the Wnt signaling pathway promotes lung cancer progression and contributes to poor patient prognosis. The porcupine inhibitor LGK974, a novel orally bioavailable cancer therapeutic in Phase I clinical trials, induces potent Wnt signaling inhibition and leads to suppressed growth and progression of multiple types of cancers. The clinical use of LGK974, however, is limited in part due to its low solubility and high toxicity in tissues that rely on Wnt signaling for normal homeostasis. Here, we report the use of host-guest chemistry to enhance the solubility and bioavailability of LGK974 in mice through complexation with cyclodextrins (CD). We assessed the effects of these complexes to inhibit Wnt signaling in lung adenocarcinomas that are typically driven by overactive Wnt signaling. 2D ^{1}H NMR confirmed host-guest complexation of CDs with LGK974. CD:LGK974 complexes significantly decreased the expression of Wnt target genes in lung cancer organoids and in lung cancer allografts in mice. Further, CD:LGK974 complexes

* Correspondence to: R. Langer Koch Institute for Integrative Cancer Research, MIT, Cambridge, MA, United States. rlanger@mit.edu (R. Langer). ** Correspondence to: M.J. Mitchell Department of Bioengineering, University of Pennsylvania, Philadelphia, PA, United States. mjmitch@seas.upenn.edu (M.J. Mitchell).

[1]Current address: Memorial Sloan Kettering Cancer Center, Cancer Biology and Genetics Program, 1275 York Avenue, New York, New York 10065, USA.

Contributions

P.P.G.G., M.T., R.L., and M.J.M. conceived the ideas, designed the experiments, interpreted the data and wrote the manuscript. P.P.P.G., M.T., T.T., K.W., A.C., K.W., R.S., and R.S.R. conducted the experiments and analyzed the data. M.O. provided assistance with mouse experiments. All authors discussed the results and commented on the manuscript.

Appendix A. Supplementary data

Supplementary data to this article can be found online at https://doi.org/10.1016/j.jconrel.2018.09.025.

increased the bioavailability upon oral administration in mice compared to free LGK974. In a mouse lung cancer allograft model, CD:LGK974 complexes induced potent Wnt signaling inhibition with reduced intestinal toxicity compared to treatment with free drug. Collectively, the development of these complexes enables safer and repeated oral or parenteral administration of Wnt signaling inhibitors, which hold promise for the treatment of multiple types of malignancies.

1. Introduction

Lung cancer is a leading cause of cancer death globally, with nonsmall cell lung cancers (NSCLCs) accounting for approximately 85% of all lung cancer cases [1]. Despite advances in early detection and standard treatment options, the 5-year relative survival rate for lung cancer is only 17%. This is due, in part, to a high proportion of patients either being metastatic at diagnosis or experiencing recurrence after initial surgery or radiotherapy [2]. Metastatic NSCLC is generally incurable, which is largely due to either intrinsic resistance to chemotherapy or acquired resistance after an initial response [3]. Therefore, there is a dire need to better understand the molecular origins of lung cancer and to develop novel therapeutic strategies to prevent and treat this disease.

The most common subtype of NSCLC is lung adenocarcinoma (LUAD), which is driven by oncogenic KRAS in approximately 30% of cases [1]. Effective chemotherapies against LUAD tumors are lacking [4]. Secreted Wnt proteins, which function in the Wnt signaling pathway that controls various biological processes throughout development and adult life, also underlie diseases such as cancer upon dysregulation of this signaling cascade. Wnt signaling is essential for the initiation and maintenance of Braf-driven lung adenomas in mice [5], and forced activation of this pathway promotes progression of Kras or Braf mutant lung tumors [5,6]. LUAD, and particularly metastasis, in humans is commonly associated with increased expression of Wnt-pathway-activating genes and downregulation of negative regulators of this pathway [7,8]. Recent studies have found that the cells in advanced mouse and human LUAD were heterogeneous and contained at least two cell subpopulations: tumor cells that respond to Wnt proteins, and a supporting cell population in tumors that express the enzyme porcupine. This enzyme adds a lipid chain to the immature form of Wnt and enables the formation of mature Wnt that is secreted from the cell [9,10]. Wnt binding to the Wnt receptor on tumor cells activated the Wnt signaling pathway, driving tumor progression and proliferative potential [9]. Interestingly, inhibition of ligand-driven Wnt signaling *via* the porcupine inhibitor LGK974, a recently discovered small molecule inhibitor [11], suppressed Wnt target genes, inhibited tumor growth and proliferation, and extended survival of mice with advanced LUAD tumors [9]. Thus, inhibition of ligand-driven Wnt signaling holds promise as a potential therapeutic strategy to treat LUAD.

The use of Wnt signaling inhibitors in cancer therapy is limited, in part, by a lack of safe and effective drug delivery systems [11,12]. Wnt signaling plays a critical role in normal tissue homeostasis, including the self-renewal process of the intestinal epithelium. Thus, oral administration of pharmacological Wnt inhibitors induces severe intestinal toxicity in mice and zebrafish [13,14]. Wnt signaling inhibition specifically *via* LGK974 oral administration induces intestinal toxicity in mice at a daily dose of 10 mg/kg [11]. Given that oral

administration is a major route of small molecule delivery, there is a major need to develop platforms that enable Wnt signaling inhibition within target cells in the tumor niche with minimal intestinal toxicity.

Cyclodextrin (CD) macrocycles are attractive candidates to improve delivery of Wnt signaling inhibitors due to their ability to form inclusion complexes with hydrophobic drugs, as well as improve their stability and solubility [15]. Incorporated in over 35 clinically approved pharmaceutical formulations [16], CDs have been shown to enhance drug absorption and oral bioavailability [17] as well as facilitate drug transport across physiologic barriers and biological membranes [18]. Furthermore, CD supramolecular affinity for a drug can prolong bioavailability, making them attractive components of controlled release formulations [19]. Herein, a library of CD:LGK974 inclusion complexes was screened for enhanced oral delivery and Wnt signaling inhibition *in vivo* (Fig. 1). A novel formulation was identified, through complexation of β-cyclodextrin sulfobutyl ethers (βSBECD) with LGK974 (βSBECD:LGK974), that enhanced LGK974 solubility and stability, increased drug bioavailability in blood upon oral administration, and induced potent Wnt signaling inhibition in LUAD tumor organoids *in vitro* and *in vivo* using genetically engineered mouse model-derived LUAD allografts.

2. Materials and methods

2.1. Isolation of primary mouse lung adenocarcinoma cells

Mice bearing KrasG12D/+; Trp53Δ/Δ;Rosa26tdTomato/+ (KPT) murine LUAD tumors were euthanized 12–26 weeks after tumor induction and perfused with S-MEM (Gibco) through the right ventricle of the heart. KPT-LUAD cells were harvested from dissected lungs and cell lines were established as described previously [9].

2.2. Cell culture

Human colon colorectal cell line Caco-2 (ATCC number HTB-37) was obtained from ATCC (Manassas, VA, USA) and cultured in EMEM medium supplemented with 20% (vol/vol) FBS and 1% (vol/vol) PenStrep. KPT-LUAD cells primary cells were cultured in Advanced DMEM/F12 supplemented with gentamicin (Thermo), penicillin-streptomycin (VWR), 10 mM HEPES (Thermo), and 2% heat-inactivated fetal bovine serum.

2.3. Reagents

Cyclodextrins (CD): α-cyclodextrin sulfobutyl ethers (αSBECD) and β-cyclodextrin sulfobutyl ethers (βSBECD) sodium salts were obtained from Ligand Pharmaceuticals, Inc. (San Diego, CA). CDs α-cyclodextrin (αCD), β-cyclodextrin (βCD) and (2-Hydroxypropyl)-β-cyclodextrin (HPβCD) were obtained from Sigma-Aldrich (Milwaukee, WI, USA). LGK974 was purchased from Selleckchem (Cambridge, MA, USA). Hydrochloric acid 37% ACS reagent, carboxymethylcellulose sodium salt (CMC), Tween-80, HPLC grade acetonitrile, trifluoroacetic acid 99% reagent plus, and dimethyl sulfoxide 99.9% ACS reagent were all obtained from Sigma-Aldrich (Milwaukee, WI, USA). Phosphate buffered saline, pH 7.4 was obtained from ThermoFisher Scientific

(Cambridge, MA, USA). Deuterium Oxide (D_2O) was obtained from Cambridge Isotope Laboratories, Inc. (Cambridge, MA, USA).

2.4. CD:LGK974 complexation

CD:LGK974 complexes were prepared in 20 mL vials at a molar ratio of 10:1 CD:LGK974 in deionized water. The reaction was stirred at room temperature and then adjusted to pH ~4–5 with 0.1 N HCl or until the solution was clear. The product was lyophilized into a dry, white powder. To measure complexation of CD:LGK974, complexes were dissolved in DMSO and measured *via* absorbance (300 nm) in a Safire absorbance plate reader from Tecan Group LTD (Männedorf, Switzerland). Results were compared against a standard curve of LGK974 in DMSO.

2.5. 2D-NMR

CD:LGK974 complexes were determined *via* 2D correlation using a 500 MHz Inova NMR from Varian, Inc. (Paolo Alto, CA, USA). Briefly, CD:LGK974 complexes were dissolved in D_2O (concentration: ~15 mg/mL) and then 2D ^1H Nuclear Overhauser effect spectroscopy (NOESY, mix time of either 400 or 650 ms, 256 FID) was performed. Complexation and structure were determined by observing the proton cross-peaks between CD (-CH-, 3–4.2 ppm) and LGK974 (aromatic –CH-, 7.7–9.2 ppm).

2.6. Isothermal titration calorimetry

Calorimetric titrations were carried out using a VP-ITC Isothermal Titration Calorimetry (ITC) Microcalorimeter (Microcal Company, Northampton, MA, USA) at 25 degrees Celsius. Each titration experiment consisted of 51 successive injections of CD (60 mM) in aqueous solution (pH 4–5) into the reaction cell charged with 1.5 mL of LGK974 (3.0 mM) in a solution of 1% DMSO, with time intervals of 300 s. The first injection (1.0 μL) was discarded to eliminate diffusion effects of material from the syringe to the reaction cell. Subsequent injections were used at a constant volume of 5.0 μL of CD. The time of injection was 2.0 s. The raw data was analyzed using the “one site model” set forth by Microcal Origin 7.0 for ITC after the subtraction of the blank experiment (CD diluted in a solution of 1% DMSO).

2.7. Caco-2 diffusion assay

Caco-2 cells were seeded on Millipore Millicell plates (Massachusetts, USA) for ~20 days to form a confluent cell monolayer prior to the experiment. On day 20, free LGK974 and CD:LGK974 complexes were added to the apical side of the membrane and the transport of the complexes across the monolayer were monitored over a 2 h time period. Ranitidine was used as low permeability control, warfarin as a high permeability control, and talinolol was used as a control to confirm that the cells are expressing efflux P-glycoprotein. Drug efflux was measured by quantifying the transport of complexes from the basolateral compartment to the apical compartment. The permeability coefficient (P_{app}) and efflux ratio were calculated from the following Eqs. (1) and (2):

$$P_{app} = \frac{dQ/dt}{C_0 \times A} \quad (1)$$

$$\text{Efflux ratio} = \frac{P_{app}(B \rightarrow A)}{P_{app}(A \rightarrow B)} \quad (2)$$

where dQ/dt is the rate of permeation of the complexes across the cells, C_0 is the donor compartment concentration at time zero and A is the area of the cell monolayer (Eq. (1)). C_0 is obtained from analysis of the dosing solution at the start of the experiment. If the P_{app} of the lucifer yellow exceeded 1×10^{-6} cm/s, it was assumed that the formation of the cell monolayer was unsuccessful or the compound exhibited cytotoxic effects. The % recovery was calculated from the following Eq. (3):

$$\%\ \text{Recovery} = \frac{\text{Total drug/complex in donor and receiver at the end of experiment (nmol)}}{\text{Initial drug/complex present(nmol)}} \times 100 \quad (3)$$

2.8. In vitro lung tumor organoid assay

150–1000 KPT-LUAD cells from established cell lines were mixed in 50% *v*/v Matrigel (BD) and 50% v/v Advanced DMEM/F12 (Gibco) and plated on 10 μL of Matrigel. The gel was allowed to solidify at 37 °C, followed by addition of Advanced DMEM/F12 supplemented with gentamicin (Thermo Fisher Scientific), penicillin-streptomycin (VWR), 10 mM HEPES (Thermo Fisher Scientific), and 2% heat-inactivated fetal bovine serum. For Wnt signaling evaluation, cultures were incubated with 100 nM LGK974 free in solution or within CD:LGK974 complexes every two days (3 treatments total) over the course of one week. To measure uptake and diffusion of calcein in organoids after CD:LGK974 treatment, the medium was removed from organoids and replaced with serum-free DMEM containing 1 μM calcein-AM (Invitrogen). Calcein uptake was observed 2 h post-treatment using fluorescence microscopy. Images were acquired using a Nikon A1R confocal microscope.

2.9. qRT-PCR

After *in vitro* and *in vivo* treatment, gene expression of *Axin2* and *Lgr5,* which are upregulated in the activated Wnt pathway and down-regulated upon Wnt signaling inhibition, was analyzed *via* qRT-PCR. For *in vitro* assays, RNA was isolated from cell or tumor samples using an RNAeasy Plus Kit (QIAGEN GmbH, Hilden, Germany) according to the manufacturer's instructions. cDNA was synthesized from 1 μg of RNA using a SuperScript VILO cDNA Synthesis Kit (Thermo Fisher Scientific). qRT–PCR was performed in triplicates with 2 μL of diluted cDNA (1:10) using PerfeCTa SYBR Green FastMix (Quanta Biosciences (Gaithersburg, MD) on a Bio-Rad iCycler qRT–PCR detection system. For *in vivo* assays, RNA was isolated using Trizol Reagent (ThermoFischer

Scientific, Cambridge, MA) according to the manufacturer's instructions. DNA was digested using RQ1 RNase-Free DNase (Promega, Madison, WI) and cDNA prepared from 2 to 5 μg RNA using GoScript™ Reverse Transcriptase Kit (Promega, Madison, WI). qRT-PCR was performed in triplicates with 1 μL undiluted cDNA using PowerUp SYBR Green Master Mix (ThermoFischer Scientific, Cambridge, MA) on Roche LightCycler 480 Instrument II. Expression was normalized to Actin or GAPDH.

Name	Sequence	Purpose
Lgr5 Fwd	CCTACTCGAAGACTTACCCAGT	qRT-PCR
Lgr5 Rev	GCATTGGGGTGAATGATAGCA	qRT-PCR
Axin2 Fwd	TGACTCTCCTTCCAGATCCCA	qRT-PCR
Axin2 Rev	TGCCCACACTAGGCTGACA	qRT-PCR
Actin Fwd	GGCTGTATTCCCCTCCATCG	qRT-PCR
Actin Rev	CCAGGTAACAATGCCATGT	qRT-PCR
Gapdh Fwd	TGGATTTGGACGCATTGGTC	qRT-PCR
Gapdh Rev	TTTGCACTGGTACGTGTTGAT	qRT-PCR

2.10. Confocal microscopy

Organoids were labeled with 10 μM EdU for 4 h, followed by the addition of 4% paraformaldehyde (Electron Microscopy Sciences) fixation for 20 min. Fluorescence-based detection of proliferating cells was performed using the Click-iT EdU Alexa Fluor 488 Imaging Kit (Invitrogen) according to the manufacturer's protocol. Images were acquired using a Nikon A1R confocal microscope.

2.11. Pharmacokinetic studies

All animal procedures were approved by the MIT Institutional Animal Care and Use Committee. Nude mice (Nu/Nu 088) were treated with 10 mg/kg/d of LGK974, CD:LGK974 complexes, or PBS via oral gavage. Blood samples (approx. 50 μL) were collected by tail bleeding at 0, 30, 60, 90, 120 and 180 min of post-dose intervals and were subsequently treated and analyzed with HPLC. All blood samples were collected in heparinized eppendorf tubes (Beckman Coulter). Blood concentrations of LGK974 were measured using an Agilent 1260 HPLC with a Kromasil C18 column (pore size: 300 A, particle size: 5 μm, 4.6 mm × 250 mm). The mobile phase is a gradient mixture of 0.1% TFA and acetonitrile (0–100%) over 19 min at 1 mL/min. Blood samples were prepared by mixing 15 μL of blood sample and 50 μL PBS, then the mixture was added to 100 μL acetonitrile in an Eppendorf tube and was incubated for 10 min. Samples were centrifuged at 10,000 RCF for 10 min, and the supernatant was removed and filtered through a 0.2 μm PTFE filter. Samples were then injected into an HPLC and the LGK974 peak measured at 300 nm absorbance. Peaks were integrated and blood concentrations were determined from a standard curve of LGK974.

For non-compartmental analysis, the area under the concentration-time curve (AUC) was calculated using a log/linear trapezoidal method from the start of the study ($t = 0$) to the last

sampling point (t = 180 min). Mean residence time (MRT) was calculated by dividing the area under the first moment concentration time curve (AUMC) by the AUC. The maximum plasma concentrations (C_{max}) were taken directly from the observed data collected from blood samples following treatment.

2.12. Wnt signaling inhibition - in vivo luminescence/fluorescence

A KPT cell line was transfected with 7TCF:Luciferase-PGK:Puro lentiviruses Addgene # 24308, which becomes positive for firefly luciferase upon activation of the Wnt pathway [20]. These cells were transplanted subcutaneously into the flanks of immunodeficient athymic nu/nu mice. One week following transplantation, mice were treated with 100 mg/kg D-Luciferin *via* I.P. administration (Perkin Elmer), and tumor burden was quantified by detecting tdTomato fluorescence using whole-animal imaging with an IVIS system (Perkin Elmer). Wnt signaling activity was quantified by normalizing the luciferase signal generated by Wnt activation to the tdTomato signal generated by the tumor burden. Imaging was performed every 24 h over the course of 1 week. Mice were treated with 5 mg/kg/d of LGK974 resuspended in 0.5% carboxymethylcellulose (Sigma) and 0.5% Tween-80 (Sigma) or CD:LGK974 complexes.

2.13. Histological analysis

Intestinal tissue was harvested from mice and fixed in 10% formalin for 24 h and was then processed for paraffin inclusion. Histological sections (5 μm thickness) were stained with hematoxylin and eosin (H& E). Intestinal toxicity was assessed in mice treated with free LGK974 or CD:LGK974 complexes at dosages of 10 mg/kg/d over 7 days, according to the following criteria: grade 0, normal mucosa villi; grade 1, development of subepithelial Gruenhagen's space at the tip of the villi; grade 2, extension of the subepithelial space with moderate epithelial lifting; grade 3, massive epithelial lifting, possibly with a few denuded villi; grade 4, denuded villi with lamina propria and exposed capillaries; and grade 5, disintegration of the lamina propria, ulceration and hemorrhage [21].

3. Results and discussion

Dysregulated activation of the Wnt signaling pathway is a key component of the proliferative potential of various cancers, and inhibition of this pathway has been shown to slow tumor growth [22]. However, the therapeutic potential of Wnt signaling inhibition has been limited due to a lack of therapeutic agents that target the Wnt signaling pathway. Recently, a potent and specific small-molecule porcupine inhibitor, LGK974, was discovered and shown to induce potent Wnt signaling inhibition [11]. LGK974 is currently in Phase I clinical trials [23] and is a potentially promising strategy for targeting Wnt-driven cancers [11]. Recently, LGK974 has been shown to inhibit lung cancer growth and prolong survival of tumor-bearing mice [9]. However, LGK974 is a hydrophobic drug that is poorly soluble in aqueous environments [11], which limits its clinical use and induces toxic effects upon administration [11,13,14]. Cyclodextrins (CD) are known to enhance both solubility and bioavailability of hydrophobic drugs by forming inclusion complexes, and they have also been used to enhance the physicochemical stability of molecules through complexation [24]. The drug LGK974 sequesters itself in the hydrophobic CD interior, while the more

hydrophilic CD exterior is exposed to the aqueous environment (Fig. 2). This enhances the solubility of LGK in aqueous solvent systems, increases *in vivo* bioavailability, and enhances Wnt inhibition of lung tumors. In addition, the ability of CDs to enhance the transport of drugs through biological membranes [17] may reduce gastrointestinal toxicity by decreasing overall drug retained in the intestinal lumen.

3.1. CD:LGK974 complexation

To improve solubility and enhance oral delivery, LGK974 was complexed with a range of CDs (αCD, αSBECD, βCD, HPβCD, βSBECD). CDs form inclusion complexes with hydrophobic drugs, improve stability and solubility [15], enhance drug absorption and oral bioavailability [17], as well as facilitate drug transport across physiological barriers and biological membranes [18]. LGK974 was complexed with CDs at a molar ratio varying between 1:1 and 1:10 (CD:LGK) in water under acidic conditions (pH = 4–5). We hypothesized that acidic conditions protonate the secondary amine on LGK974 (non-ionized form) and enable complexation with CDs. LGK974 was less hydrophobic when deprotonated at higher pH, and this ionized form did not readily complex with CDs. All CD:LGK974 complexes were soluble in aqueous solution except for βCD:LGK974, due to the known low solubility of unmodified βCD [25]. However, modified βCDs (HPβCD and βSBECD) formed soluble complexes with LGK974 due to the presence of hydrophilic 2-hydroxypropyl or sulfobutyl ether groups on CDs, respectively. In most cases, the interactions between host and guest molecules occur by guest insertion through its less polar part into the CD cavity. The more polar and charged group is placed outside of the host cavity, and thus is exposed to the bulk solvent to interact with the hydroxyl or sulfobutyl ether groups. Both of these groups increase the hydrophilicity of βCD, but the sulfobutyl ether modification shows greater complexation strength. We speculate that this is because the sulfobutyl ether has a nonpolar 4 carbon alkane portion that can interact with hydrophobic drugs through Van-Der-Waals forces. Alternatively, the shorter 2-hydroxypropyl lacks an equivalent nonpolar region for this interaction, resulting in a weaker complexation.

To characterize the host-guest interactions and to gain insight into the molecular interactions between CDs and LGK974, 2D NOESY NMR was performed (Fig. 3). 2D NOESY NMR provides data consisting of intermolecular NOE correlations between hydrogens of different species [26]. Intense cross peaks were found between aromatic hydrogens of LGK974, and H3 and H5 hydrogens located in the CD cavity. Analysis of the cross-peaks demonstrated structural differences between the α- and βCD complexes (Fig. 3a). The βCD complexes had more interactions with LGK974 than the αCD complexes, likely due to their larger ring size (Fig. 3b–c). Based on 2D NMR, an inclusion arrangement of the aromatic rings of LGK974 inside the CD cavity is likely (Fig. 3b–c). These results indicate that CDs and LGK974 effectively form supramolecular complexes. These complexes are soluble in water and could be an alternative to the standard preparation for oral gavage, which requires surfactants and sonication to produce a suspension that remains insoluble [9,11,27,28].

In addition to the spectroscopic methods described here, further theoretical studies, such as the semi-empirical method and the density functional theory (DFT), would provide valuable

information on the formation of the inclusion complexes. Further, these studies can predict the most probable and stable arrangements of the complexes [26]. These theoretical calculations are important to assess the molecular mechanics of the CD:LGK974 complexes and to demonstrate a variety of guest inclusion possibilities to predict the most stable CD:LGK974 complexes.

3.2. Complexation constant, stoichiometry, and complexation enthalpies

The interaction mechanisms of CDs with LGK974 were studied using isothermal titration calorimetry (ITC). ITC measures the thermodynamic changes of host-guest interactions, such as CD:drug complexes, and determines the strength of interaction (complexation constant) and stoichiometry in solution [29,30]. The average stoichiometry N of the complex in solution and its thermodynamic parameters of interaction (enthalpy ΔH°, entropy ΔS°, complexation constant $K_{complex}$) were determined.

The sigmoidal profile obtained for the titration process allowed the fitting of the experimental data to a Wiseman isotherm and showed the molar partial enthalpy of injection ($\Delta_{inj}H°$) of the CD. In this experiment, 60.0 mM CD was added into 1.5 mL of 10 mM citrate buffer (blank) or into 1.5 mL of 3.0 mM LGK974 (titration) (Fig. 4). An equivalence point at a molar ratio of approximately $N = 1.18$ for HPβCD:LGK974 and $N = 0.664$ for βSBECD:LGK974 in the sigmoid curves suggested the occurrence of a 1:1 stoichiometry; however, this does not necessarily exclude the possible existence of other stoichiometries for the inclusion complexes at chemical equilibrium.

Based on the 1:1 stoichiometry, the complexation constant calculated from the ITC experiments, $K_{complex1:1}$, which refers to the formation of a CD:LGK974 complex, can be described by Eq. (4):

$$\mathrm{CD + LGK974} \overset{K_{complex1:1}}{\rightleftharpoons} \mathrm{CD{:}\ LGK974} \qquad (4)$$

$$K_{complex1:1} = [\mathrm{CD{:}\ LGK974}]/[\mathrm{CD}][\mathrm{LGK974}]$$

The interaction between βSBECD and LGK974 is an exothermic process cooperatively accompanied by an entropy increase, leading to an especially strong interaction between the two species ($K_{complex1:1} = 1720 \pm 156\ M^{-1}$) compared to other CD:guest systems [29–31]. The interaction between HPβCD and LGK974 is also an exothermic process, but the complexation constant ($K_{complex1:1} = 170 \pm 5.49\ M^{-1}$) is measured to be 10 times lower than that of βSBECD:LGK974, indicating a weaker host:guest interaction. The stronger intermolecular interactions may be due to stronger intermolecular interactions of LGK974 with the sulfobutyl ether groups on βSBECD compared with the hydroxypropyl groups on HPβCD. The positive entropy change for both is associated to the high desolvation of the molecules with a consequent gain of translational and rotational degrees of freedom by the water molecules [29]. Collectively, these data along with the NMR results suggest the spontaneous formation of CD:LGK974 supramolecular complexes.

3.3. Caco-2 permeability assay

To assess the absorption of drugs across intestinal epithelium, we measured the transport of LGK974 and CD:LGK974 complexes across monolayers of the Caco-2 intestinal epithelial cell line (Fig. 5). The Caco-2 cell assay is an established *in vitro* model used to determine the permeability of compounds and to predict their oral absorption *in vivo* [32]. Apical to basolateral (A → B) and basolateral to apical (B → A) permeability across Caco-2 monolayers was investigated for CD:LGK974 complexes and free LGK974. Both free LGK974 and CD:LGK974 exhibited high permeability across Caco-2 monolayers, despite the low solubility of LGK974. The permeation of the drug across Caco-2 monolayers (B → A) was increased following complexation with CD in comparison to free LGK974, which resulted in a significant increase of the efflux ratio of CD:LGK974 (Fig. 5) ($P < .05$, $P < .01$). However, all CD:LGK974 complexes have an efflux ratio lower than 1 and are not subject to active efflux. The integrity of monolayers was tested by measuring transepithelial electrical resistance (TEER) with lucifer yellow transport as a control [33]. The TEER values did not decrease significantly after treatments with free drug or CD complexes, indicating that the treatment was nontoxic to Caco-2 monolayers. In summary, these results demonstrate that CD:LGK974 complexes showed high bidirectional permeability across Caco-2 epithelial monolayers, with minimal toxicity to intestinal epithelial cells.

3.4. In vitro organoid Wnt inhibition

The Wnt signaling pathway is crucial for the maintenance of the proliferative potential of lung adenocarcinomas [9]. Active Wnt signaling induces the transcription of Axin2 and Lgr5, and the suppression of these transcripts is indicative of Wnt inhibition [34,35]. To assess the effect of CD:LGK974 treatment on Wnt inhibition *in vitro*, we isolated primary KPT-LUAD cells and established low-density 3-dimensional (3D) tumor organoids (Fig. 6), which better recapitulate Wnt signaling *in vivo* [9]. CD:LGK974 complexes were able to suppress Wnt signaling activation at a concentration of 100 nM. KPT-LUAD organoids treated with CD:LGK974 had decreased expression of Axin2 transcripts compared to PBS-treated controls (Fig. 6a). However, there was no significant difference in Axin2 (Fig. 6a) and Lgr5 (Fig. 6b) transcripts between CD:LGK974 complexes and free LGK974 treatment *in vitro*. Collectively, these results indicate that CD:LGK974, specifically βSBECD:LGK974 and HPβCD:LGK974, induce potent Wnt signaling inhibition in tumor organoids *in vitro*.

3.5. Diffusion in CD:LGK974 treated organoids

We hypothesized that potent Wnt signaling inhibition in CD:LGK974 treated tumor organoids was due to enhanced permeation of LGK974 throughout the organoids, as CDs have been shown to enhance drug transport across biological barriers and membranes. To investigate whether CD:LGK974 enhances drug uptake and diffusion in organoids, CD:LGK974 treated KPT-LUAD organoids were labeled with calcein-AM, a substrate of the efflux transporter P-glycoprotein, that is used to quantify drug uptake and diffusion in 3D cell culture [36]. Uptake and diffusion of calcein-AM was enhanced after treatment with CD:LGK974 complexes compared to free drug (Fig. 6d–e). Of note, βSBECD:LGK974 and HPβCD:LGK974 treatment significantly increased Calcein-AM uptake in KPT-LUAD

organoids compared to other treatment conditions (Fig. 6d–e). Increased Calcein-AM uptake in organoids due to CD treatment could be due to two factors: modulation of P-glycoprotein drug efflux pumps on tumor cells, and tumor cell membrane instability. Treatment with CDs has been shown to negatively modulate P-glycoprotein drug efflux pumps in enterocytes [37]. Given that P-glycoproteins are overexpressed in a range of solid tumor types and contribute to drug resistance [38,39], it is possible that CD:LGK974 treatment increases uptake in tumor cells by negatively modulating P-glycoprotein drug efflux pumps. In terms of permeability, CDs have been shown to induce cell plasma membrane instability through the removal of hydrophobic compounds such as cholesterol [40–42]. Therefore, CD:LGK974 treatment could potentially induce membrane instability in tumor organoids, thereby increasing drug uptake. Future studies will investigate the mechanisms of CD:LGK974 intracellular delivery.

3.6. Pharmacokinetic studies

To investigate the *in vivo* bioavailability of LGK974 or CD:LGK974 complexes, nu/nu mice were treated *via* oral gavage at 10 mg/kg with free LGK974, αSBECD:LGK974, HPβCD:LGK974 or βSBECD:LGK974. Blood samples were collected over the course of 120 min post-injection and were analyzed by HPLC using the absorbance at 300 nm. Blood concentrations were measured using the area under the curve (AUC) and were plotted as a line graph (Fig. 7a). Mice treated with either HPβCD:LGK974 or βSBECD:LGK974 showed significantly increased LGK974 concentrations in blood ($P < .05$) compared to mice treated with free LGK974 or αSBECD:LGK974 at 30–60 min post-injection. Further, the calculated AUC and AUMC of both HPβCD:LGK974 and βSBECD:LGK974 were more than two times higher than free LGK974, as reported in the supplementary material (Table S1). These results suggest that these modified CD complexes substantially increase LGK974 oral bioavailability, which could reduce the dosages necessary to inhibit Wnt signaling and reduce intestinal toxicity.

3.7. Wnt signaling inhibition - in vivo luminescence/fluorescence

To investigate the effect of CD drug complexes on Wnt inhibition *in vivo*, mice bearing allograft KPT-LUAD tumors were treated with free LGK974, HPβCD:LGK974, or βSBECD:LGK974 *via* oral gavage administration. Mice bearing allograft KPT-LUAD tumors were used, as it was previously shown that the Wnt pathway is activated in autochthonous KPT-LUAD tumors *in vivo* [9]. In this regimen, mice were treated with a 5 mg/kg/d dose of LGK974 over 1 week. *In vivo* treatment with CD:LGK974, in particular βSBECD:LGK974, significantly reduced expression of Wnt target genes Axin2 (Fig. 7e) and Lgr5 (Fig. 7f) compared to free LGK974 ($P < .05$ and $P < .001$, respectively) and control treatments ($P < .001$).

Wnt signaling inhibition was also measured in mice bearing allograft KPT-LUAD tumors *via* whole-animal bioluminescence imaging. Treatment with CD:LGK974 complexes induced Wnt signaling inhibition as measured *via* decreased bioluminescence (Fig. 7 b-d). Specifically, βSBECD:LGK974 treatment significantly reduced bioluminescence in tumor-bearing mice compared to free LGK974 and PBS-treated mice ($P < .05$ and $P < .001$, respectively), which is indicative of reduced Wnt signaling. βSBECD:LGK974 treatment

significantly reduced *in vivo* bioluminescence compared to all other treatment regimens (Fig. 7 b-d), possibly due to a stronger host:guest interaction that enhances drug transport across the intestinal barrier.

3.8. In vivo toxicity

Wnt signaling is essential for intestinal tissue homeostasis and epithelial tissue regeneration [43]. While LGK974 treatment has been shown to be well-tolerated at lower dosages, continuous, high dosing of LGK974 may induce loss of intestinal epithelium *in vivo* [11,27]. We hypothesized that CD:LGK974 complexes reduce LGK974-induced intestinal toxicity upon oral administration. To assess the degree of intestinal toxicity due to CD:LGK974 treatment, mice were treated with free LGK974 or CD:LGK974 complexes at dosages of 10 mg/kg/d over a 7 day period, after which the intestinal mucosal damage was evaluated *via* histopathological scoring [21]. Intestinal mucosal damage was observed in mice treated with free LGK974 (Fig. 8), but CD:LGK974 complexes were well-tolerated without significant intestinal damage at identical dosages (Fig. 8, $P < .001$). These experiments suggest that CDs reduce the intestinal toxicity associated with high doses of LGK974. While the exact mechanism behind reduced toxicity requires further studies, the high binding strength of βSBECD to LGK974 could potentially reduce direct interactions between the drug and the intestinal epithelium. Additionally, enhanced drug transport across this barrier due to drug complexation with CDs could reduce the amount of drug remaining within the intestine, thereby reducing overall intestinal toxicity [18].

4. Conclusion

The development of CD:LGK974 complexes *via* host-guest chemistry enhanced oral delivery and induced potent Wnt signaling inhibition in lung cancer organoids and in tumor-bearing mice, with reduced toxicity compared to free drug. CD:LGK974 complexes increased LGK974 bioavailability and enhanced Wnt signaling inhibition in mice bearing lung adenocarcinoma allografts. The exact mechanism behind increased bioavailability and inhibition of Wnt signaling *in vivo via* the lead CD:LGK974 complex, βSBECD:LGK974, will require further study. However, we speculate that increased bioavailability and Wnt signaling inhibition with this complex is potentially due to stronger interactions with LGK974 compared to other CDs, which was confirmed *via* ITC. Stronger interactions between LGK974 and βSBECD could serve to (i) enhance drug transport across the intestinal barrier, thereby increasing drug bioavailability and uptake in tumors, (ii) shield the drug from direct interactions with the intestinal epithelium, to reduce toxicity and enabling higher dosing, and (iii) reduce the amount of drug remaining within the intestine upon oral administration.

While the current study investigated Wnt signaling inhibition in mice bearing allograft lung tumors, the development of CD:LGK974 complexes could enable more continuous and higher doses of Wnt signaling inhibitors in a range of mouse models of cancer with reduced side effects compared to free drug. This would enable further fundamental studies on the role of Wnt signaling in cancer progression *in vivo.* Given that LGK974 is currently being evaluated in phase I clinical trials [23], the development of these complexes could

potentially enable safer, repeated oral or parenteral administration of Wnt inhibitors to lung tumors *in vivo*, as a means to treat lung cancer either alone or in combination with therapeutics currently utilized in the clinic.

Supplementary Material

Refer to Web version on PubMed Central for supplementary material.

Acknowledgements

M.J.M. was supported by a Burroughs Wellcome Fund Career Award at the Scientific Interface, a National Institutes of Health (NIH) Director's New Innovator Award (DP2TR002776), and a grant from the American Cancer Society (129784-IRG-16-188-38-IRG). R.S.R. was support by an NIH T32 Multidisciplinary Traning grant. This work was supported in part by a Cancer Center Support (core) Grant P30-CA14051 from the National Cancer Institute, and a grant from the Koch Institute's Marble Center for Cancer Nanomedicine (to R.L.). We thank K. Cormier and C. Condon from the Koch Institute Swanson Biotechnology Center Histology Facility and L. A. Orellano from the Department of General Pathology, Institute of Biological Sciences, Universidade Federal de Minas Gerais for histology support. P.P.G.G. was supported by Leslie Misrock Cancer Nanotechnology Postdoctoral Fellowship.

References

[1]. Herbst RS, Heymach JV, Lippman SM, Lung cancer, N. Engl. J. Med 359 (2009) 1367–1380, 10.1056/NEJMra0802714.

[2]. Siegel RL, Miller KD, Jemal A, Cancer statistics, 2016, CA Cancer J. Clin 66 (2016) 7–30, 10.3322/caac.21332. [PubMed: 26742998]

[3]. Stewart DJ, Tumor and host factors that may limit efficacy of chemotherapy in non-small cell and small cell lung cancer, Crit. Rev. Oncol. Hematol 75 (2010) 173–234, 10.1016/j.critrevonc.2009.11.006. [PubMed: 20047843]

[4]. Johnson DH, Schiller JH, Bunn PA, Jr., Recent clinical advances in lung cancer management, J. Clin. Oncol 32 (2016) 973–982, 10.1200/JCO.2013.53.1228.

[5]. Juan J, Muraguchi T, Iezza G, Sears RC, McMahon M, Diminished WNT → β-catenin → c-MYC signaling is a barrier for malignant progression of BRAFV600Einduced lung tumors, Genes Dev. 28 (2014) 561–575, 10.1101/gad.233627.113. [PubMed: 24589553]

[6]. Pacheco-Pinedo EC, Durham AC, Stewart KM, Goss AM, Lu MM, Demayo FJ, et al., Wnt/β-catenin signaling accelerates mouse lung tumorigenesis by imposing an embryonic distal progenitor phenotype on lung epithelium, J. Clin. Invest 121 (2011) 1935–1945, 10.1172/JCI44871. [PubMed: 21490395]

[7]. Stewart DJ, Wnt Signaling Pathway in Non–Small Cell Lung Cancer, J. Natl. Cancer Inst 106 (2014) djt356, 10.1093/jnci/djt356. [PubMed: 24309006]

[8]. Nguyen DX, Chiang AC, Zhang XHF, Kim JY, Kris MG, Ladanyi M, et al., WNT/TCF Signaling through LEF1 and HOXB9 Mediates Lung Adenocarcinoma Metastasis, Cell 138 (2009) 51–62, 10.1016/j.cell.2009.04.030. [PubMed: 19576624]

[9]. Tammela T, Sanchez-Rivera FJ, Cetinbas NM, Wu K, Joshi NS, Helenius K, et al., A Wnt-producing niche drives proliferative potential and progression in lung adenocarcinoma, Nature 545 (2017) 355–359, 10.1038/nature22334. [PubMed: 28489818]

[10]. Lim JS, Ibaseta A, Fischer MM, Cancilla B, O'Young G, Cristea S, et al., Intratumoural heterogeneity generated by Notch signalling promotes small-cell lung cancer, Nature 545 (2017) 360–364, 10.1038/nature22323. [PubMed: 28489825]

[11]. Liu J, Pan S, Hsieh MH, Ng N, Sun F, Wang T, et al., Targeting Wnt-driven cancer through the inhibition of Porcupine by LGK974, Proc. Natl. Acad. Sci. U. S. A 110 (2013) 20224–20229, 10.1073/pnas.1314239110. [PubMed: 24277854]

[12]. Mitchell MJ, Jain RK, Langer R, Engineering and physical sciences in oncology: challenges and opportunities, Nat. Rev. Cancer 17 (2017) 659–675, 10.1038/nrc.2017.83. [PubMed: 29026204]

[13]. Lau T, Chan E, Callow M, Waaler J, Boggs J, Blake RA, et al., A novel tankyrase small-molecule inhibitor suppresses APC mutation–driven colorectal tumor growth, Cancer Res. 73 (2013) 3132–3144, 10.1158/0008-5472.CAN-12-4562. [PubMed: 23539443]

[14]. Chen B, Dodge ME, Tang W, Lu J, Ma Z, Fan C-W, et al., Small molecule–mediated disruption of Wnt-dependent signaling in tissue regeneration and cancer, Nature Chem. Biol 5 (2009) 100–107, 10.1038/nchembio.137. [PubMed: 19125156]

[15]. Webber MJ, Langer R, Drug delivery by supramolecular design, Chem. Soc. Rev 27 (2017) 89, 10.1039/C7CS00391A.

[16]. Kurkov SV, Loftsson T, Cyclodextrins, Int. J. Pharm 453 (2013) 167–180, 10.1016/j.ijpharm.2012.06.055. [PubMed: 22771733]

[17]. Carrier RL, Miller LA, Ahmed I, The utility of cyclodextrins for enhancing oral bioavailability, J. Control. Release 123 (2007) 78–99, 10.1016/j.jconrel.2007.07.018. [PubMed: 17888540]

[18]. Loftsson T, Brewster ME, Pharmaceutical applications of cyclodextrins: effects on drug permeation through biological membranes, J. Pharm. Pharmacol 63 (2011) 1119–1135, 10.1111/j.2042-7158.2011.01279.x. [PubMed: 21827484]

[19]. Hirayama F, Cyclodextrin-based controlled drug release system, Adv. Drug Deliv. Rev 36 (1999) 125–141, 10.1016/S0169-409X(98)00058-1. [PubMed: 10837712]

[20]. Fuerer C, Nusse R, Lentiviral vectors to probe and manipulate the Wnt signaling pathway, PLoS One 5 (2010) e9370, 10.1371/journal.pone.0009370. [PubMed: 20186325]

[21]. Chiu C-J, McArdle AH, Brown R, Scott HJ, Gurd FN, Intestinal mucosal lesion in low-flow states: I. a morphological, hemodynamic, and metabolic reappraisal, Arch. Surg 101 (1970) 478–483, 10.1001/archsurg.1970.01340280030009. [PubMed: 5457245]

[22]. Polakis P, Wnt Signaling in Cancer, Cold Spring Harb. Perspect. Biol 4 (2012) a008052, 10.1101/cshperspect.a008052. [PubMed: 22438566]

[23]. U.S. National Library of Medicine. A Study of LGK974 in Patients With Malignancies Dependent on Wnt Ligands ClinicalTrials.gov, https://clinicaltrials.gov/ct2/show/NCT01351103?term=lgk974&rank=1 (accessed November 15, 2017).

[24]. Loftsson T, Brewster ME, Pharmaceutical applications of cyclodextrins. 1. Drug solubilization and stabilization, J. Pharm. Sci 85 (2017) 1017–1025, 10.1021/js950534b.

[25]. Muller B, Brauns U, Solubilization of drugs by modified β-cyclodextrins, Int. J. of Pharm 26 (1985) 77–88, 10.1016/0378-5173(85)90201-7.

[26]. De Sousa FB, Denadai AML, Lula IS, Nascimento CS, Fernandes Neto NSG, Lima AC, et al., Supramolecular self-assembly of cyclodextrin and higher water soluble guest: thermodynamics and topological studies, J. Am. Chem. Soc 130 (2008) 8426–8436, 10.1021/ja801080v. [PubMed: 18529008]

[27]. Moon J, Zhou H, Zhang L-S, Tan W, Liu Y, Zhang S, et al., Blockade to pathological remodeling of infarcted heart tissue using a porcupine antagonist, Proc. Natl. Acad. Sci. U. S. A 114 (2017) 1649–1654, 10.1073/pnas.1621346114. [PubMed: 28143939]

[28]. Zhang L-S, Lum L, Delivery of the porcupine inhibitor WNT974 in Mice, Wnt Signaling, Humana Press, New York, NY, 2016, pp. 111–117, 10.1007/978-1-4939-6393-5_12.

[29]. Gontijo SML, Guimarães PPG, Viana CTR, Denadai ÂML, Gomes ADM, Campos PP, et al., Erlotinib/hydroxypropyl-β-cyclodextrin inclusion complex: characterization and in vitro and in vivo evaluation, J. Incl. Phenom. and Macrocycl. Chem 83 (2015) 267–279, 10.1007/s10847-015-0562-3.

[30]. Connors KA, The stability of cyclodextrin complexes in solution, Chem. Rev 97 (1997) 1325–1358, 10.1021/cr960371r. [PubMed: 11851454]

[31]. Suárez DF, Consuegra J, Trajano VC, Gontijo SML, Guimarães PPG, Cortés ME, et al., Structural and thermodynamic characterization of doxycycline/ β-cyclodextrin supramolecular complex and its bacterial membrane interactions, Colloids Surf. B Biointerfaces 118 (2014) 194–201, 10.1016/j.colsurfb.2014.01.028. [PubMed: 24816509]

[32]. Hubatsch I, Ragnarsson EGE, Artursson P, Determination of drug permeability and prediction of drug absorption in Caco-2 monolayers, Nature Protoc. 2 (2007) 2111–2119, 10.1038/nprot.2007.303. [PubMed: 17853866]

[33]. Fenyvesi F, Réti-Nagy K, Bacsó Z, Gutay-Tóth Z, Malanga M, Fenyvesi É, et al., Fluorescently labeled methyl-beta-cyclodextrin enters intestinal epithelial Caco-2 cells by fluid-phase endocytosis, PLoS One 9 (2014) e84856, 10.1371/journal.pone.0084856. [PubMed: 24416301]

[34]. Jho EH, Zhang T, Domon C, Joo CK, Freund JN, Costantini F, Wnt/-catenin/ Tcf signaling induces the transcription of Axin2, a negative regulator of the signaling pathway, Mol. Cell. Biol 22 (2002) 1172–1183, 10.1128/MCB.22.4.1172-1183.2002. [PubMed: 11809808]

[35]. Clevers H, Loh KM, Nusse R, An integral program for tissue renewal and regeneration: Wnt signaling and stem cell control, Science 346 (2014) 1248012, 10.1126/science.1248012. [PubMed: 25278615]

[36]. Achilli T-M, McCalla S, Meyer J, Tripathi A, Morgan JR, Multilayer spheroids to quantify drug uptake and diffusion in 3D, ACS Nano 11 (2014) 2071–2081, 10.1021/mp500002y.

[37]. Rong W-T, Lu P, Tao Q, Guo M, Lu Y, Ren Y, et al., Hydroxypropyl-sulfobutyl-β-cyclodextrin improves the oral bioavailability of edaravone by modulating drug efflux pump of enterocytes, J. Pharm. Sci 103 (2014) 730–742, 10.1002/jps.23807. [PubMed: 24311389]

[38]. Fojo AT, Ueda K, Slamon DJ, Poplack DG, Gottesman MM, Pastan I, Expression of a multidrug-resistance gene in human tumors and tissues, Proc. Natl. Acad. Sci. U. S. A 84 (1987) 265–269, 10.1073/pnas.84.1.265. [PubMed: 2432605]

[39]. Szakács G, Paterson JK, Ludwig JA, Booth-Genthe C, Gottesman MM, Targeting multidrug resistance in cancer, Nat. Rev. Drug Discov 5 (2006) 219–234, 10.1038/nrd1984. [PubMed: 16518375]

[40]. Kilsdonk EPC, Yancey PG, Stoudt GW, Bangerter FW, Johnson WJ, Phillips MC, et al., Cellular cholesterol efflux mediated by cyclodextrins, J. Biol. Chem 270 (1995) 17250–17256, 10.1074/jbc.270.29.17250. [PubMed: 7615524]

[41]. Zidovetzki R, Levitan I, Use of cyclodextrins to manipulate plasma membrane cholesterol content: evidence, misconceptions and control strategies, Biochim. Biophys. Acta 1768 (2007) 1311–1324, 10.1016/j.bbamem.2007.03.026. [PubMed: 17493580]

[42]. Ahsan F, Arnold JJ, Yang T, Meezan E, Schwiebert EM, Pillion DJ, Effects of the permeability enhancers, tetradecylmaltoside and dimethyl-β-cyclodextrin, on insulin movement across human bronchial epithelial cells (16HBE14o−), Eur. J. Pharm. Sci 20 (2003) 27–34, 10.1016/S0928-0987(03)00163-5. [PubMed: 13678790]

[43]. Crosnier C, Stamataki D, Lewis J, Organizing cell renewal in the intestine: stem cells, signals and combinatorial control, Nat. Rev. Gene 7 (2006) 349–359, 10.1038/nrg1840.

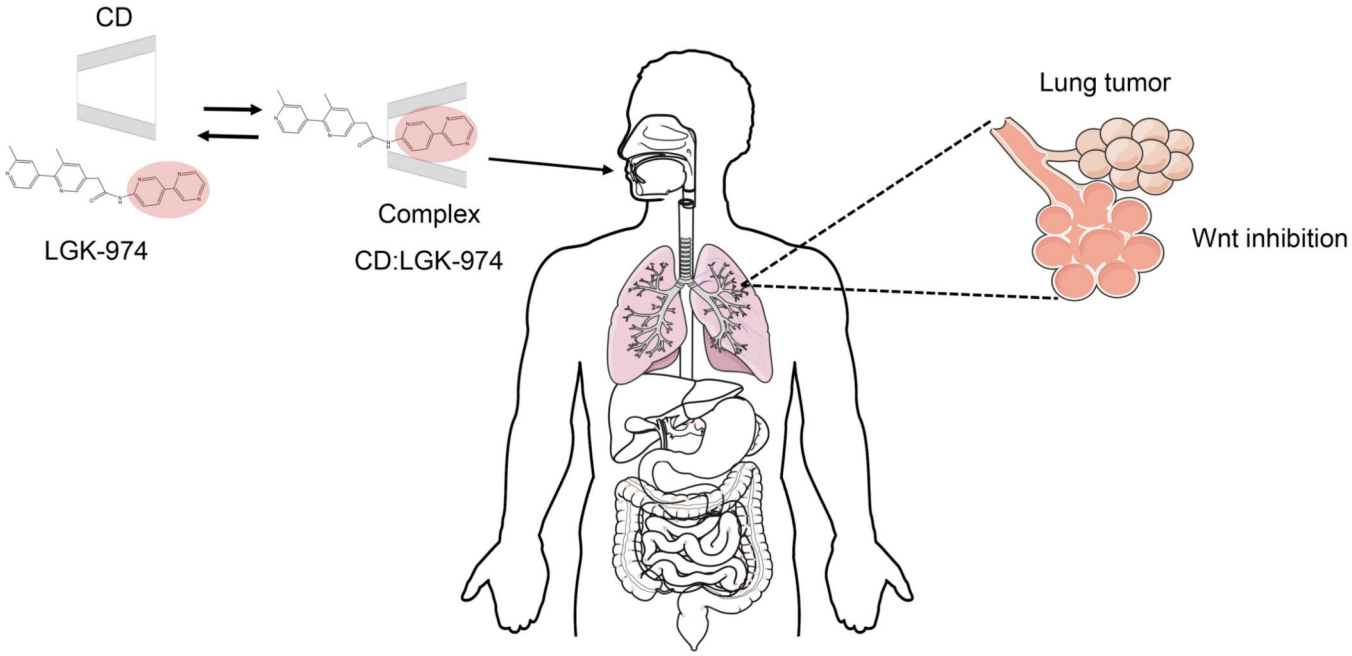

Fig. 1.
Schematic of CD:LGK974 complexation for oral delivery of Wnt inhibitors *in vivo*.

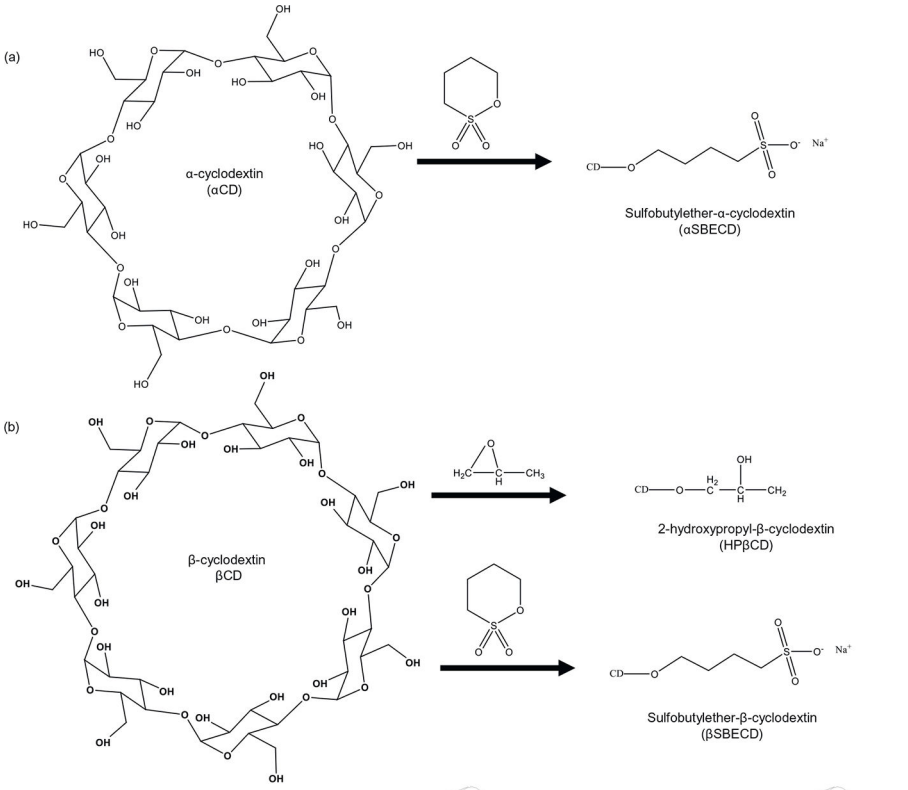

(d)

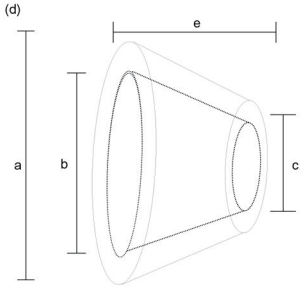

Property	αCD	αSBECD	βCD	HPβCD	βSBECD
# of glucose units	6	6	7	7	7
Molecular weight	9.73	9.73	11.35	11.35	11.35
External diameter (a)	13.7 Å	13.7 Å	15.3 Å	15.3 Å	15.3 Å
Internal diameter (b)	5.7 Å	5.7 Å	7.8 Å	7.8 Å	7.8 Å
Internal diameter (c)	4.4 Å	4.4 Å	5.8 Å	5.8 Å	5.8 Å
Height (e)	7.8 Å	7.8 Å	7.8 Å	7.8 Å	7.8 Å
Cavity volume	174 $Å^3$	174 $Å^3$	262 $Å^3$	262 $Å^3$	262 $Å^3$
Water solubility	1.45 g/L	>500 g/L	0.19 g/L	>500 g/L	~700 g/L

Fig. 2.

(a) Structure of α-cyclodextrin and modified sulfobutylether-α-cyclodextrin. (b) Structure of β-cyclodextrin and modified sulfobutylether-β-cyclodextrin. (c) Scheme of reversible host-guest complex formation. (d) Table of physicochemical properties of cyclodextrins.

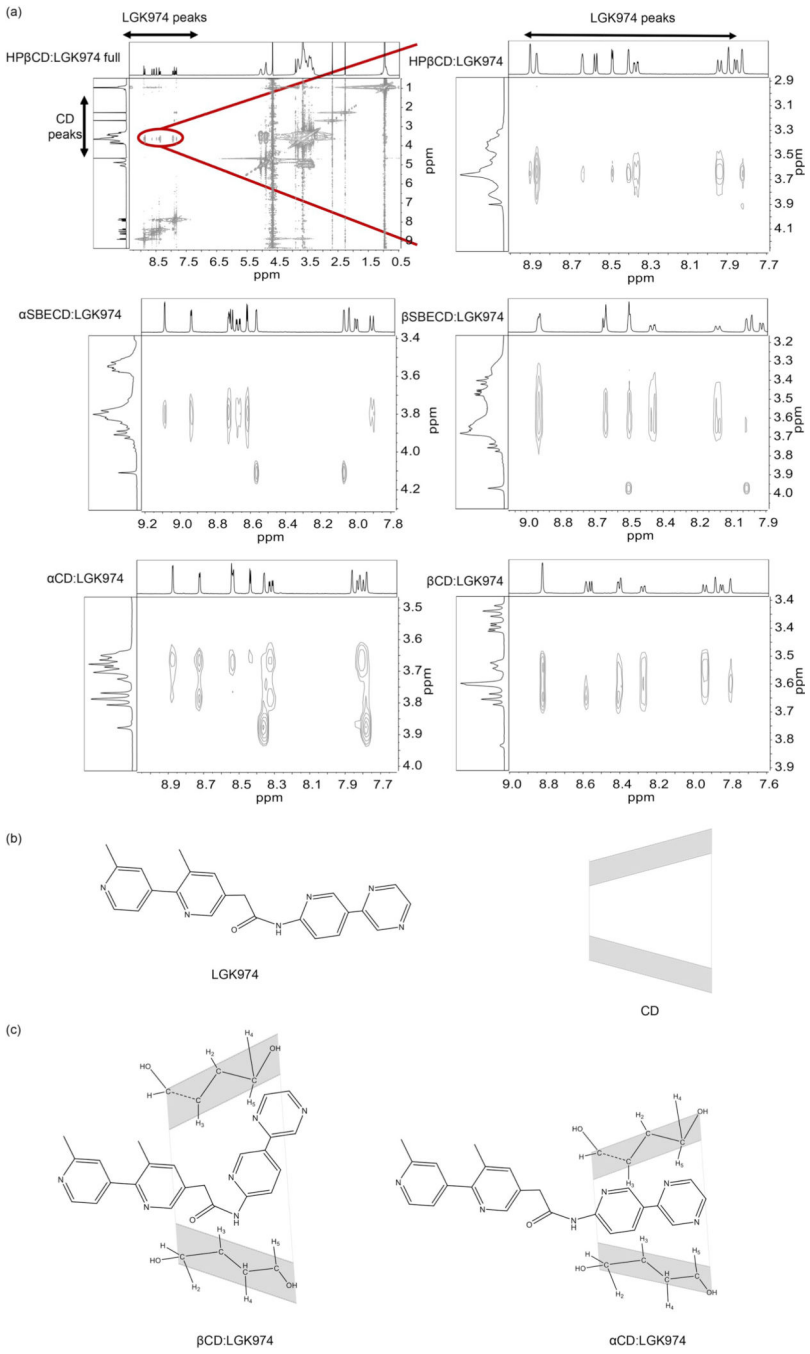

Fig. 3.

(a) Partial 2D NOESY NMR spectrum of CD:LGK974. (b,c) Proposed geometric arrangement of LGK974 in the cavities of HPβCD and βSBECD based on the ROESY experiment.

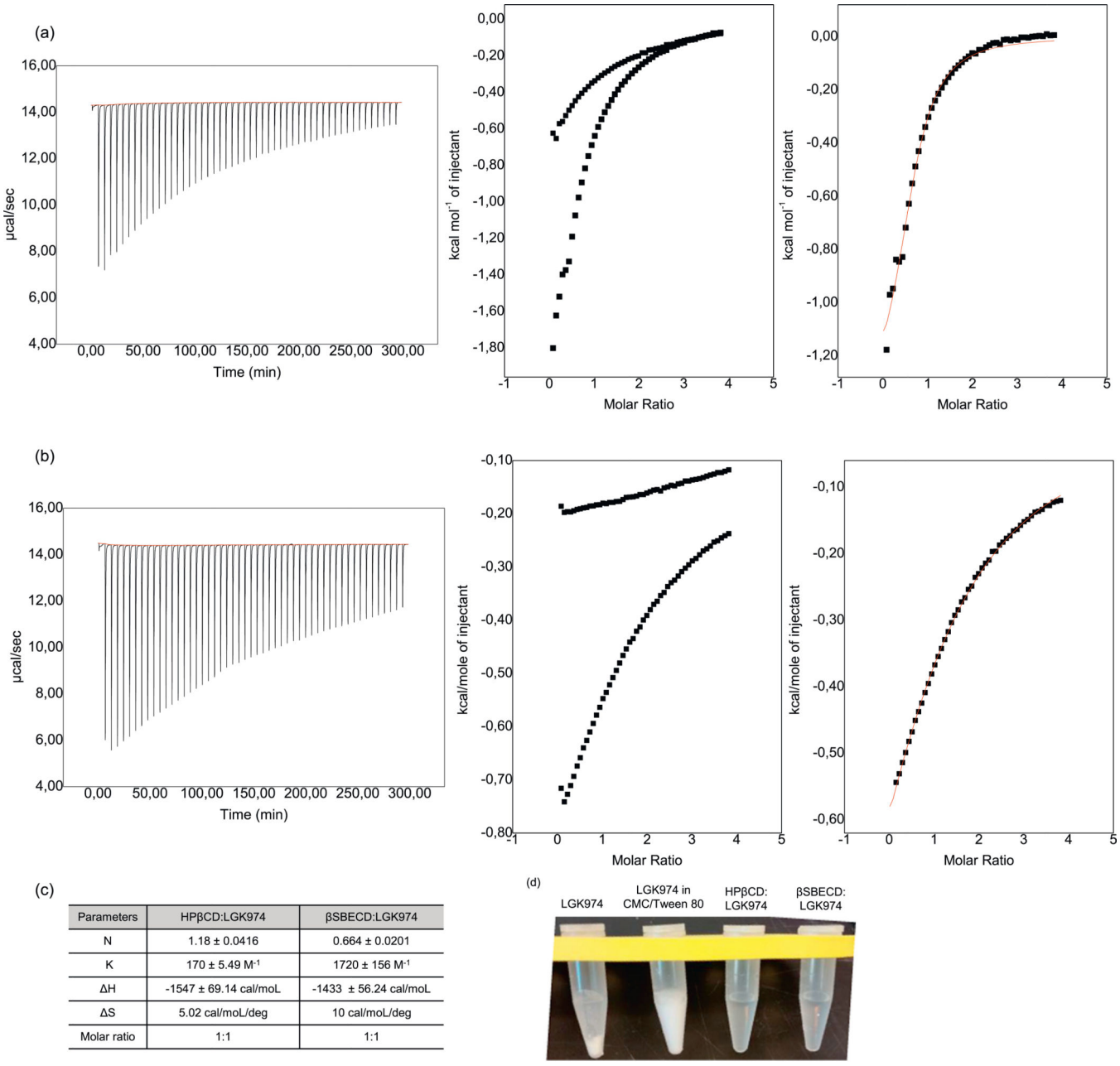

Parameters	HPβCD:LGK974	βSBECD:LGK974
N	1.18 ± 0.0416	0.664 ± 0.0201
K	170 ± 5.49 M^{-1}	1720 ± 156 M^{-1}
ΔH	-1547 ± 69.14 cal/moL	-1433 ± 56.24 cal/moL
ΔS	5.02 cal/moL/deg	10 cal/moL/deg
Molar ratio	1:1	1:1

Fig. 4.

Isothermal Titration Calorimetry experiments for (a) βSBECD (concentration: 60.0 mM) and (b) HPβCD (concentration: 60.0 mM) in LGK974 (concentration: 3.0 mM) (square) and nonlinear fitting by Wiseman Isotherm (line). (c) Thermodynamic parameters of CD-LGK974 interactions determined by isothermal titration calorimetry experiments (average stoichiometry N of the complex in solution, enthalpy ΔH°, entropy TΔS°, equilibrium constant K_{eq}). (d) Free LGK974, LGK974 suspension in CMC/Tween 80 and CD:LGK974 solubility in PBS.

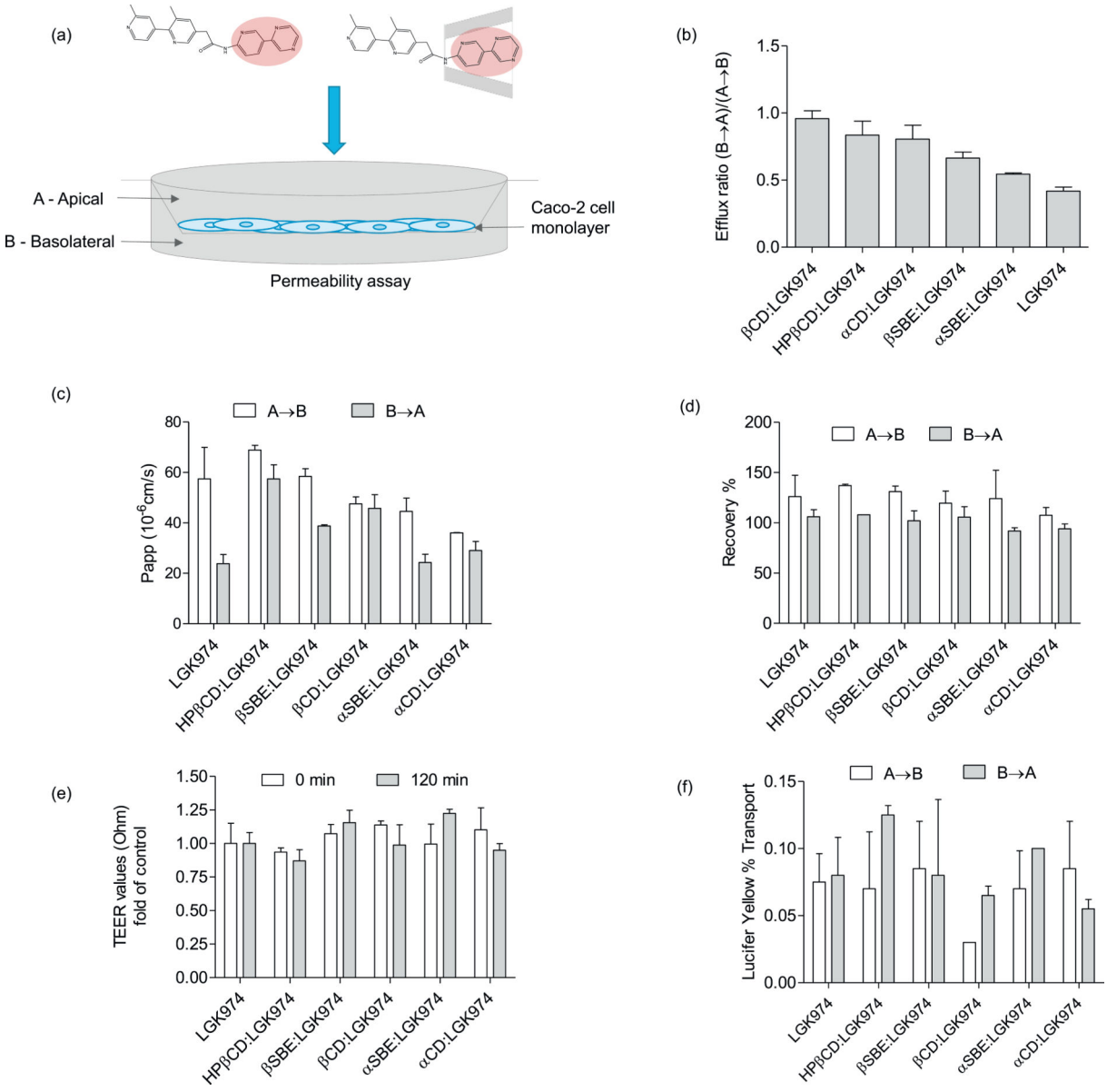

Fig. 5.

(a) Schematic of the Caco-2 drug permeability assay. (b) Efflux ratio, (c) permeability coefficient (Papp), (d) experimental recovery, (e) transepithelial electrical resistance (TEER) and (f) lucifer yellow percentage of LGK974 and CD:LGK974 complexes after 2 h treatment.

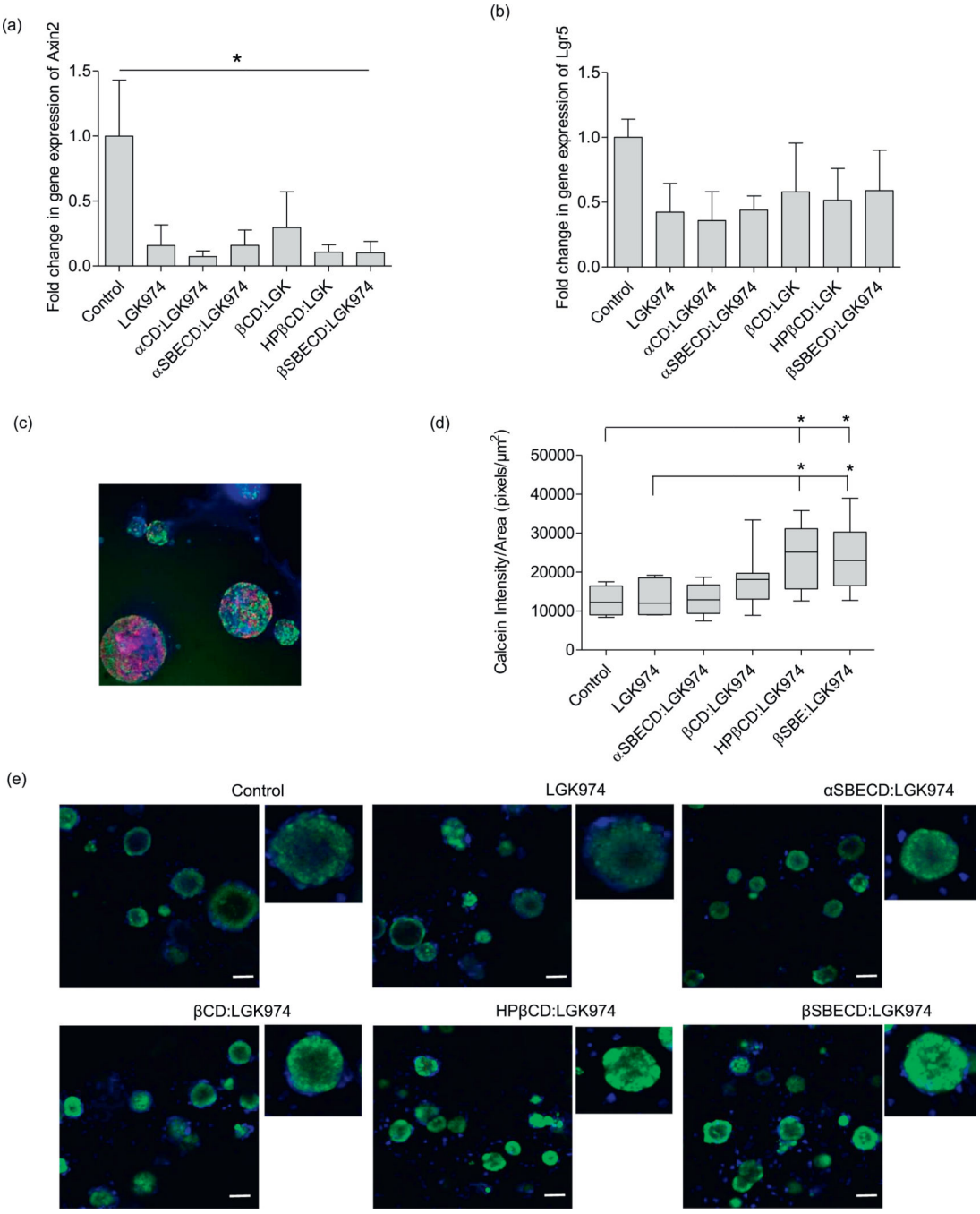

Fig. 6.

Quantitative real-time PCR (qRT-PCR) analysis of (a) *Axin2* and (b) *Lgr5* transcripts in 3D cultures of primary *KPT*- LUAD cells following Wnt pathway inhibition with LGK974 or CD:LGK974 treatment (concentration: 100nM) every two days (three treatments total) over the course of one week. (c) Immunofluorescence staining for EdU (green), BrdU (red), and nuclei (blue) in 3D cultures of primary *KPT*- LUAD cells. (d) Calcein pixel intensity by organoid area of LGK974 and CD:LGK974 complexes. (e) Uptake and diffusion of fluorescent calcein in *KPT*- LUAD organoids after treatment with LGK974 and

CD:LGK974. Organoids were incubated with 1μM calcein-AM and fluorescent images were taken 2h after incubation at 37 °C and 10% CO_2. Data are mean ± s.d.; one-way ANOVA with posthoc Bonferri (b); * $P < .05$; ** $P < .01$; *** $P < .001$ compared to control group. (For interpretation of the references to colour in this figure legend, the reader is referred to the web version of this article.)

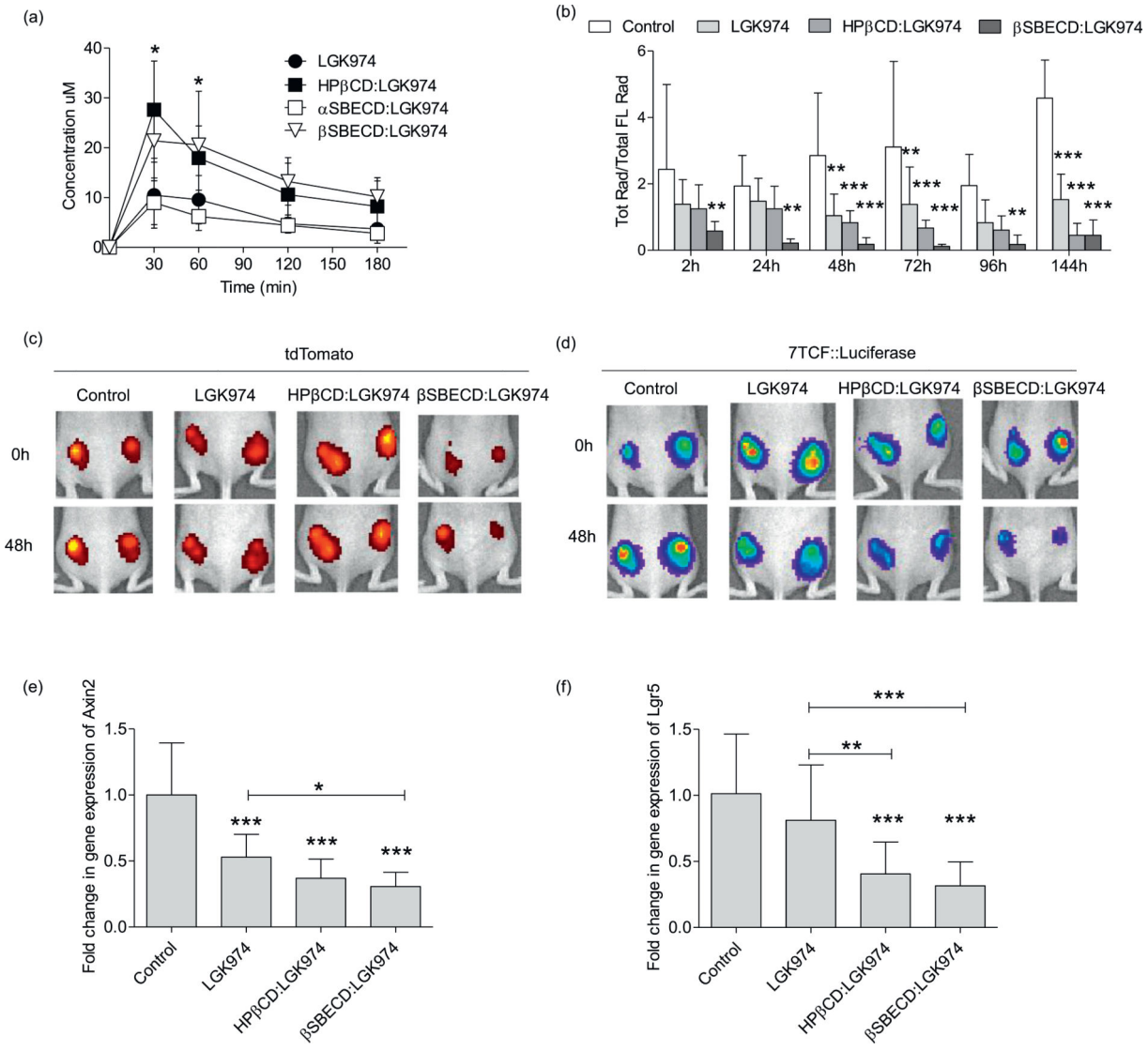

Fig. 7.

(a) Blood concentration of LGK974 between 30 min and 180 min after oral administration of LGK974 and CD:LGK974 (dose: 10 mg/kg). (b) Suppression of 7TCF-driven bioluminescence by LGK974 or CD:LGK974 relative to tdTomato signal in mice harboring subcutaneous transplants of the KPT LUAD cell line. Treatment with 5mg/kg/d of LGK974 or CD:LGK974 over 7days, n =8 tumors, 4 mice per group. (c, d) tdTomato and 7TCF::Luciferase signals at baseline (0 h) and 48 h following treatment with LGK974 or CD:LGK974 complexes (dose: 5mg/kg). Quantitative real-time PCR analysis of (e) *Axin2* and (f) *Lgr5* transcripts in *KPT*-LUAD tumors 1 week following treatment with 5mg/kg/d LGK974 or CD:LGK974. Treatment was started at 1week post-tumor initiation. Data are mean ± s.d.; Two-way ANOVA (a, b); One-way ANOVA (e,f) * P < .05; ** P < .01; *** P < .001 compared to control (b, e, f) and LGK974 group (a, e, f).

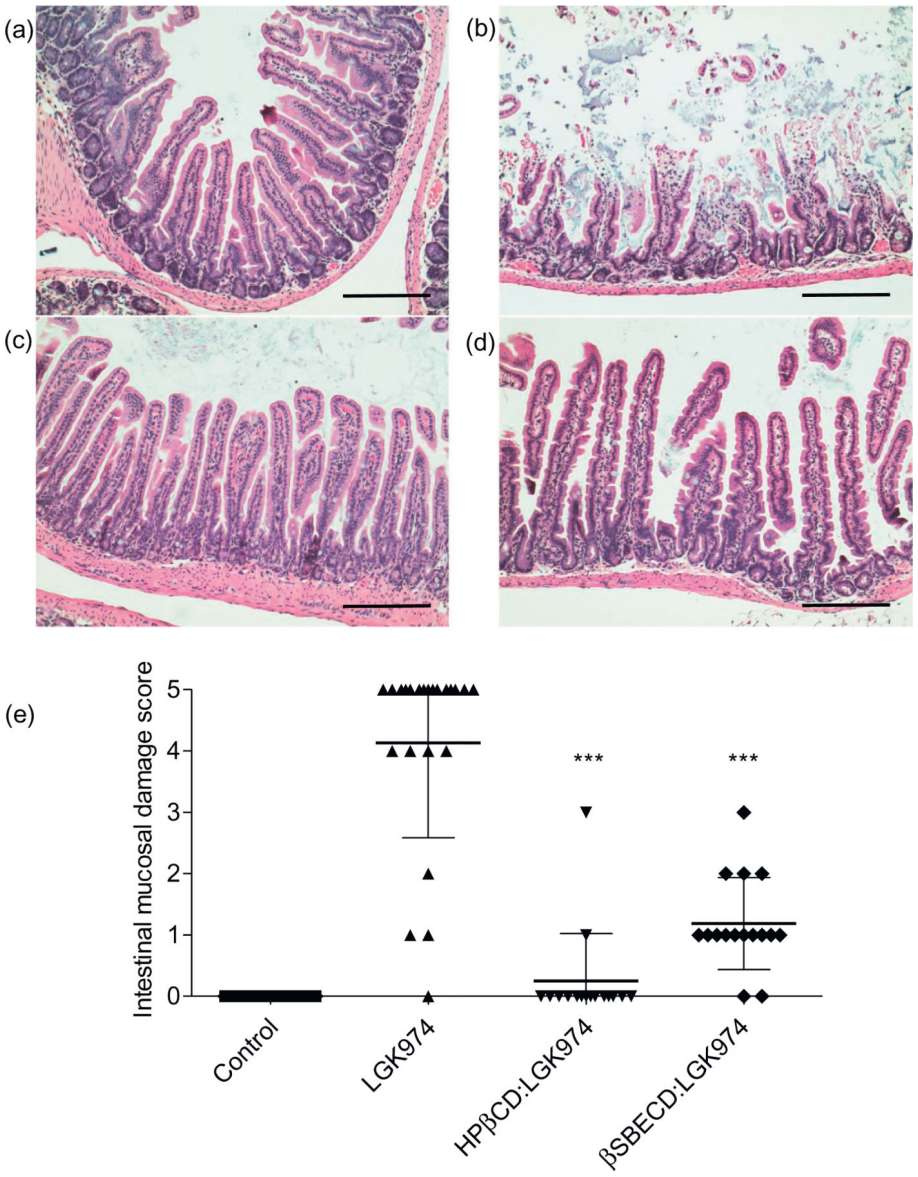

Fig. 8.

Representative images of H&E staining of the intestine from mice treated with (a) PBS, (b) LGK974, (c) HPβCD:LGK974, or (d) βSBECD:LGK974 complexes at high dosages of 10mg/kg/d over 7days (Magnification: duodenum, 20×.Scale bars: 20×−100 μm. (e) Scoring for intestinal mucosal damage. *** $P < .001$ compared to the LGK974 group.